# Bundling of Actin Filaments by Elongation Factor 1 α Inhibits Polymerization at Filament Ends

**John W. Murray, Brian T. Edmonds, Gang Liu, and John Condeelis**

Department of Anatomy and Structural Biology, Albert Einstein College of Medicine, Bronx, New York 10461

***Abstract.*** Elongation factor 1 α (EF1α) is an abundant protein that binds aminoacyl-tRNA and ribosomes in a GTP-dependent manner. EF1α also interacts with the cytoskeleton by binding and bundling actin filaments and microtubules. In this report, the effect of purified EF1α on actin polymerization and depolymerization is examined. At molar ratios present in the cytosol, EF1α significantly blocks both polymerization and depolymerization of actin filaments and increases the final extent of actin polymer, while at high molar ratios to actin, EF1α nucleates actin polymerization. Although EF1α binds actin monomer, this monomer-binding activity does not explain the effects of EF1α on actin polymerization at physiological molar ratios. The mechanism for the inhibition of polymerization is related to the actin-bundling activity of EF1α. Both ends of the actin filament are inhibited for polymerization and both bundling and the inhibition of actin polymerization are affected by pH within the same physiological range; at high pH both bundling and the inhibition of actin polymerization are reduced. Additionally, it is seen that the binding of aminoacyl-tRNA to EF1α releases EF1α's inhibiting effect on actin polymerization. These data demonstrate that EF1α can alter the assembly of F-actin, a filamentous scaffold on which nonmembrane-associated protein translation may be occurring in vivo.

ELONGATION factor 1 α (EF1α)[1] is an essential component of the protein synthetic machinery but is expressed in molar excess to its known ligands in the protein synthetic machinery, such as specific aminoacyl-tRNAs and elongation factor β/γ (Slobin, 1980). EF1α has been isolated as an actin-binding and -bundling protein from *Dictyostelium* originally named ABP-50 (Demma et al., 1990). Sequence analysis demonstrates that ABP-50 is *Dictyostelium* EF1α and is capable of catalyzing protein synthesis in vitro (Yang et al., 1990). The discovery that EF1α binds actin with nano- to micromolar affinity in physiological buffers (Dharmawardhane et al., 1991; Bektas et al., 1994; Edmonds et al., 1995) and is present at a cytosolic molar ratio of 1:4 for EF1α/actin suggests that most of the EF1α within cells should be associated with actin. Indeed, EF1α is found associated with the actin cytoskeleton by immunofluorescence (Dharmawardhane et al., 1991; Collings et al., 1994; Edmonds et al., 1995, 1996) and electron microscopy (Bassell et al., 1994*a*; Liu et al., 1996*a*). Antibodies to EF1α coprecipitate actin from whole cell extracts in approximately a 1:2 molar ratio of EF1α/actin. Additionally, it has been shown that EF1α binds actin monomer that is cross-linked to Sepharose beads (Dharmawardhane et al., 1991).

Much of the protein synthetic machinery, including EF1α, is found in association with the actin cytoskeleton (for review see Condeelis, 1995). The consequences of the interaction of the protein synthetic machinery with actin is unknown. It appears that the protein synthetic machinery does not exist in a freely diffusing form in eukaryotic cells (Stapulionis and Deutscher, 1995), and many reports have been published on the transport and anchorage of mRNA on the actin cytoskeleton (Bassell et al., 1994*b*). EF1α, EF1-β (personal communication, Marcus Fechheimer, University of Georgia), EF-2, mRNA, and ribosomes are also associated with the actin cytoskeleton as shown in vivo by immunofluorescence, electron microscopy, in situ hybridization, and in vitro by biochemical methods (Zambetti et al., 1990*a*,*b*; Dharmawardhane et al., 1991; Shestakova et al., 1993; Bassell et al., 1994*a*; Bektas et al., 1994). Actin appears to provide a means to transport and anchor this nondiffusible machinery in specific regions of a cell and this in turn may localize protein product (Kislauskis et al., 1994). Actin filaments may also participate in the channeling of essential metabolites during polypeptide elongation (Condeelis, 1995).

EF1α is the most abundant component of the protein synthetic machinery and a very abundant actin-binding protein. Therefore, its ability to influence the assembly

Address all correspondence to John Condeelis, Department of Anatomy and Structural Biology, Albert Einstein College of Medicine, 1300 Morris Park Ave., Bronx, NY 10461. Tel.: (718) 430-4068. Fax: (718) 518-7236.

1. *Abbreviations used in this paper:* PME, polymerization buffer; EF1α, elongation factor 1 α.

and structure of the actin cytoskeleton could be a key event in the transport, anchorage, and translation of mRNA. In this paper, we explore the effects of EF1α on actin polymerization and filament stability.

## Materials and Methods

### Protein and Aminoacyl-tRNA Purification

All reagents were purchased from Sigma Chemical Co. (St. Lois, MO) unless otherwise noted. *Dictyostelium* EF1α was purified according to published methods (Edmonds et al., 1995). Rabbit and *Dictyostelium* actin were purified as described previously (Condeelis and Vahey, 1982; Bresnick and Condeelis, 1991) and pyrene-labeled according to published methods (Hall et al., 1989). Unless otherwise noted, experiments used *Dictyostelium* actin. Actin was stored in the monomeric form in dialysis in buffer A (2 mM Tris, 0.2 mM $CaCl_2$, 0.2 mM ATP, 0.5 mM DTT, 0.02% $NaN_3$, pH 8.0). EF1α was stored in liquid nitrogen in α storage buffer (20 mM Pipes, 1 mM DTT, 0.02% $NaN_3$, 25% glycerol, pH 7.0).

The method that we used to synthesize [$^3$H]Phe-tRNA is essentially the same as that reported by Schreier et al. (1977), except that we used tRNA stocks rich in $tRNA^{Phe}$. tRNA synthetases were isolated from rabbit reticulocyte lysates (Promega Corp., Madison, WI) by centrifugation at 95,000 rpm for 20 min at 4°C (model TLA-100; Beckman Instrs., Fullerton, CA). The pellet was resuspended and then centrifuged in a buffer containing 20 mM Tris, pH 7.5, 1 mM DTT, 0.1 mM EDTA, 0.25 M sucrose, and 0.5 M KCl. Supernatants contained tRNA synthetases. For each bulk preparation, a small scale tRNA aminoacylation was conducted to optimize conditions. Usually 80–90% of $tRNA^{Phe}$ was aminoacylated based on the amount of [$^3$H]Phe incorporation.

EF1α was bound to GTP and GDP by incubation with 1 mM GTP or GDP for 30 min at room temperature in α storage buffer containing 5 mM $MgCl_2$. Nucleotide binding was confirmed by nitrocellulose filtration assay or mant-GTP fluorescence (Nagata et al., 1976; Liu et al., 1996). Binding of EF1α-GTP to Phe-tRNA was performed by incubating 5.7 μM Phe-tRNA with 7.1 μmM EF1α-GTP (in a solution with 1 mM GTP to reduce EF1α's binding to GDP, which is produced by the GTPase activity of EF1α) for 10 min before mixing with actin. Formation of ternary complex was confirmed under nearly identical conditions by intrinsic tryptophan fluorescence, GTPase assays, and Sephadex G75 gel filtration (Bagshaw and Harris, 1987; Crechet and Parmeggiani, 1987; Nagata et al., 1976; Slobin and Moller, 1976; Liu et al., 1996).

### Polymerization Assays

Polymerization buffer (PME) contained 20 mM Pipes, 2 mM EGTA, 2 mM $MgCl_2$, 1 mM ATP, 1 mM DTT, 0.02% $NaN_3$, 50 mM KCl, and 50 nM free calcium. If not otherwise specified, PME was at pH 6.5. This buffer contains physiological concentrations of monovalent salts that have been measured in amebas as ~50 mM (Marin and Rothman, 1980). Small volumes of buffer A and α storage buffer enter the reactions along with G-actin and EF1α. A constant free calcium concentration was maintained by adjusting 10× PME stocks according to conditions prescribed by a metal chelation computer program incorporating EGTA/EDTA, $H^+$, nucleotide, and divalent cation concentrations (from Dr. Toshikazu Hamasaki, Albert Einstein College of Medicine). Because potassium hydroxide was added to raise the pH, the final solutions were brought to the same ionic strength by addition of potassium chloride as confirmed by electrical conductivity. At equal conductivity, a total of 50 mM potassium had been added to the buffers as both KOH and KCl. Other variations (e.g., small differences in glycerol concentration) were compensated for using α storage buffer controls.

Polymerization of actin was monitored by pyrene (5–10% labeled) fluorescence (excitation 365 nm, emission 407 nm) using either an SLM8000 (SLM/Aminco, Urbana, IL) or a Hitachi F2000 fluorimeter (Mountain View, CA). In unseeded polymerization experiments, actin polymerization was initiated by the addition of pyrene actin to a cuvette containing PME buffer and either EF1α or α storage buffer. In seeded polymerization experiments, 1.5 μM G-actin and various concentrations of EF1α (or control buffer) were incubated for 3 min, at which time 0.5 μM of sheared (by vortexing) actin filaments were added to the cuvette. In depolymerization experiments, EF1α (or control buffer) was added to aliquots of F-actin 3 min before dilution. Depolymerization was initiated by a 50-fold dilution of 1.5 μM F-actin into PME buffer containing predilution concentrations of EF1α or control buffer. Polymerization and depolymerization rates were determined by the slope of a linear regression to the first 20 s of the reaction. The reactions were performed at 22°C or room temperature.

### Gelsolin-capped Filaments

5 μm actin was polymerized with 0.2 μM gelsolin (a generous gift from Dr. Toshi Azuma, Brigham and Women's Hospital, Boston MA) in a buffer containing 2 mM Tris, pH 7.5, 1 mM $MgCl_2$, 0.02% $NaN_3$, 10 mM KCl, and 100 μM $CaCl_2$. This was used as a 10× stock of seeds to start polymerization reactions as above. After equilibration to steady state (18 h), the fluorescence from these reactions was used in Fig. 6 *c*. PME buffer was adjusted to 100 μM $CaCl_2$ in steady-state experiments using various concentrations of gelsolin (Fig. 6, *a* and *b*) to ensure that the gelsolin was fully active.

### Monomer Binding

We followed a procedure similar to that of Lee and Pollard (1988). A cuvette containing the maximal concentration of EF1α and 0.05 μM pyrene actin was repeatedly diluted into 0.05 μM pyrene actin, 1× PME, and the proper amount of α storage buffer to ensure that the only constituent changing during the dilution was EF1α. After a 2-min equilibration pause, the fluorescence was measured at excitation 344 nm and emission 386 nm. In addition, we measured light scattering at 344 nm, which produced a linear signal versus EF1α concentration and assured us that nothing (such as inner-filter effects or other technical problems) was interfering with the excitation signal. The data of Fig. 3 were fit (Origin computer software; Microcal Inc., Northampton, MA) to a bimolecular binding isotherm according to the expression:

$$Y = \frac{X}{Kd + X} \times P1 + P2, \quad (1)$$

where $Y$ equals the fraction of bound actin, $X$ equals the free EF1α concentration, and $P1$ and $P2$ are standardizing variables ($P1$ is the maximal change and $P2$ is the background value). The maximal change in fluorescence was set to 1 and the data were replotted as fractional approach to this number as shown in Fig. 4.

Some monomer-binding experiments contained 0.1 μM DNAse (Worthington Biochemical Corp., Freehold, NJ) whose actin binding activity was confirmed in actin polymerization experiments (not shown). The magnitude of fluorescence change in the monomer-binding assay was compared to a standard curve for F-actin pyrene fluorescence under identical conditions. The maximal fluorescence associated with the binding of 0.05 μM actin monomer gave a signal that was equivalent to the polymerization of 0.003 μM pyrene actin.

### Mechanisms for the Inhibition of Actin Polymerization by EF1α

***Monomer-sequestering Mechanism.*** A curve showing the effect of EF1α on actin polymerization if EF1α were sequestering actin monomers (Fig. 5 *a*) was generated using a monomer binding equilibrium expression (2) and the actin polymerization rate expression (3).

The monomer binding equilibrium expression:

$$K_d mon = \frac{[G\text{-}actin]\ [EF1\alpha]}{[EF1\alpha \cdot G\text{-}actin]} \quad (2)$$

Substituting the total protein concentrations:

$$K_d mon = \frac{([G\text{-}actin]_{tot} - [EF1\alpha \cdot G\text{-actin}]) \times ([EF1\alpha]_{tot} - [EF1\alpha \cdot G\text{-actin}])}{[EF1\alpha \cdot G\text{-actin}]}$$

This quadratic equation was solved to determine the amount of $[EF1\alpha \cdot G\text{-}actin]$ at each experimental concentration of $(EF1\alpha)_{tot}$ with the help of Mathcad computer software (version 3.1; MathSoft Inc., Cambridge, MA) and using the $K_d mon$ (1.4 μM) generated from the monomer binding studies (see Fig. 4).

The actin polymerization rate expression for the barbed end is:

$$Rate_{actin} = [Filament\ End] \times (k_+ [G\text{-actin}] - k_-) \text{ (Pollard, 1983)} \quad (3)$$

In the presence of a monomer sequestering EF1α this becomes:

$$Rate_{\text{Actin + EF1}\alpha} = [Filament\ End] \times (k_+([G\text{-actin}] - [EF1\alpha \cdot G\text{-actin}]) - k_-) \quad (4)$$

The percent inhibition of the initial rate of actin polymerization (see Fig. 5 *a*) is calculated according to the expression:

$$\frac{Rate_{\text{Actin}} - Rate_{\text{Actin + EF1}\alpha}}{Rate_{\text{Actin}}} \times 100\% \quad (5)$$

where $Rate_{\text{Actin}}$ is the polymerization rate in the absence of EF1α and $Rate_{\text{Actin + EF1}\alpha}$ is the polymerization rate in the presence of EF1α.

In the presence of a monomer-sequestering EF1α, this reduces to:

$$\frac{[EF1\alpha \cdot G\text{-}actin]}{[G\text{-}actin]_{tot} - \frac{k_-}{k_+}} \times 100\% \quad (6)$$

Eq. 6 was solved for the concentrations shown in Fig. 5 *a* using a value of 0.1 μM for $k_-/k_+$ (the actin barbed-end critical concentration).

To generate a curve for the dimer sequestering model (where EF1α binds two actin monomers), we assumed complete independence for the two binding sites and therefore solved the monomer binding equations (above) with twice as much $[EF1\alpha]_{total}$.

***Capping Mechanism.*** A curve showing the effect of EF1α on actin polymerization if EF1α were capping both ends of an actin filament was generated using an end-capping equilibrium expression (we assume rapid equilibrium) (Eq. 7) and the actin polymerization rate expression (Eq. 3).

$$K_{d_{cap}} = \frac{[End]\,[EF1\alpha]}{[EF1\alpha \cdot End]} \quad (7)$$

where. $[End] = [End]_{tot} - [End - EF1\alpha]$. Substituting this into Eq. 7, we get

$$\frac{[EF1\alpha \cdot End]}{[End]_{tot}} = \frac{[EF1\alpha]}{K_d + [EF1\alpha]}. \quad (8)$$

Note that Eq. 8 is in the form of a standard binding isotherm such as Eq. 1. In this case, the total concentration of EF1α is about 1,000-fold greater than the concentration of filament ends and therefore, $[EF1\alpha] \approx [EF1\alpha]_{total}$.

In the presence of our hypothetical capping protein that caps both ends of the actin filament with the same affinity, the actin polymerization rate expression (3) becomes:

$$Rate_{\text{Actin + EF1}\alpha} = ([End]_{tot} - [EF1\alpha \cdot End]) \times (k_+[G\text{-}actin] - k_-) \quad (9)$$

and the percent inhibition of actin polymerization (Eq. 5) reduced to:

$$\frac{[EF1\alpha \cdot End]}{[End]_{tot}}.$$

This is the same as the left side of Eq. 8, and therefore we modeled the activity of a capping protein using the bimolecular binding isotherm of Eq. 1.

***Bundling Mechanism.*** The curve showing the effect of EF1α on actin polymerization (see Fig. 5 *a*) if EF1α were inhibiting actin polymerization through a bundling mechanism was generated by considering two features: bundling and end-burying. The bundling feature assumes that an actin filament must contain a certain amount of bound EF1α to rapidly form bundles, that is, to become a bundle-competent filament. The end-burying feature assumes that filament ends within a bundle become buried (hidden from solution and/or annealed) at a particular rate as the bundles form.

In Fig. 5 *a*, the inhibition of actin polymerization is plotted as a function of the total amount of EF1α. Using the $K_d$ for the binding of EF1α to F-actin of Edmonds et al. (1995) (assuming rapid equilibrium), we calculated the amount of EF1α bound to F-actin ($[EF1\alpha\text{–}F\text{-}actin]$) for various concentrations of $[EF1\alpha]_{total}$ using the F-actin binding equilibrium expression:

$$K_{d_{F\text{-}actin}} = \frac{[F\text{-}actin]\,[EF1\alpha]}{[EF1\alpha \cdot F\text{-}actin]}. \quad (10)$$

Substituting the total protein concentrations:

$$K_{d_{F\text{-}actin}} = \frac{([F\text{-}actin]_{tot} - [EF1\alpha \cdot F\text{-}actin]) \times ([EF1\alpha]_{tot} - [EF1\alpha \cdot F\text{-}actin])}{[EF1\alpha \cdot F\text{-}actin]}$$

Using the light scattering data of Fig. 5 *b* and Eq. 10, we calculated that the amount of EF1α bound to F-actin required to give a rate of bundle formation >0 was ~0.31 bound EF1α per F-actin subunit (0.25 μM $[EF1\alpha]_{tot}$, 0.5 μM $[F\text{-}actin]_{tot}$). We took the value of 0.31 to be the overall ratio of bound F-actin subunits to total F-actin subunits required for bundle formation. To determine the distribution of filaments that would have enough bound EF1α to be bundle competent, we used Bernoulli's probability distribution and considered that the F-actin behaves statistically like a collection of filament helical crossovers, or 13 monomer subunits.

The Bernoulli equation (e.g., Feynman et al., 1963):

$$\frac{n!}{k!\,(n-k)!} \times p^k \times q^{(n-k)} \quad (11)$$

If the population of helical crossovers each contain $n = 13$ subunits, then this equation gives the expected fraction of helical crossovers that would contain $k$ bound subunits given an overall total fraction of $p$ bound subunits; that is, $p$ is the overall fraction of bound F-actin subunits, $q$ is the overall fraction of unbound F-actin subunits $(1-p)$, $n$ is the total number of F-actin subunits in a helical crossover, and $k$ is the number of bound subunits in the crossover. Therefore, to determine the fraction of helical crossovers that are expected to have at least 0.31 bound F-actin subunits per total F-actin subunits (4 bound F-actin subunits per 13 total F-actin subunits), we summed the frequencies of finding <4 bound F-actin subunits per 13 total F-actin subunits for any given overall fraction of bound F-actin subunits (from Eq. 10) and subtracted this from 1, i.e., we set $n = 13$, and $k = 0, 1, 2, 3$. The fraction of bundle-competent filaments (BCF) is then:

$$1 - \sum_k \left\{ \frac{13!}{k!\,(13-k)!} \times \left( \frac{[EF1\alpha \cdot F\text{-}actin]}{[F\text{-}actin]_{tot}} \right)^{(k)} \times \left( 1 - \frac{[EF1\alpha \cdot F\text{-}actin]}{[F\text{-}actin]_{tot}} \right)^{(13-k)} \right\} \quad (12)$$

We found by increasing the shear of free filaments as well as by increasing the molar ratios of gelsolin to actin in gelsolin-capped filaments that a greater number concentration of filament ends caused a greater inhibition of actin polymerization by EF1α. Because a first-order loss-of-filament-end rate constant does not account for this, we used a second-order rate constant similar to the annealing mechanism of Kinosian et al. (1993). The rate of change in the number of filament ends per second (ignoring any back reaction) can be given by:

$$-[BCF \cdot End]^2 k_{bundle} \quad (13)$$

Integrating Eq. 13 with respect to time, the number of bundle-competent filament ends at time $t$ =

$$\frac{[BCF \cdot End]_{(0)}}{k_{bundle} \times t \times [BCF \cdot End]_{(0)} + 1} \quad (14)$$

where $[BCF - End]$ = Eq. 12 × $[End]_{total}$. $[End]_{total}$ is the number concentration (0.6 nM), measured using the known ATP barbed end polymerization rate constants (Pollard and Cooper, 1986) and the calibrated polymerization rate.

The rate of actin polymerization in the presence of EF1α is then:

$$Rate_{\text{Actin + EF1}\alpha} = \left( [Ends]_{unbundled} + \frac{[BCF \cdot End]_{(0)}}{k_{bundle} \times t \times [BCF \cdot End]_{(0)} + 1} \right) \times (k_+[G\text{-}actin] - k_-) \quad (15)$$

and the inhibition of actin polymerization (5) in the presence of EF1α reduces to:

$$\left\{ 1 - \left( \frac{[End]_{unbundled} + \frac{[BCF \cdot End]_{(0)}}{k_{bundle} \times t \times [BCF \cdot End]_{(0)} + 1}}{[End]_{tot}} \right) \right\} \times 100\%. \quad (16)$$

$t$ is the time at which the polymerization rate is measured (20 s). The rate constant for burying the filament ends that best approximated the observed data was 250 $\mu M^{-1}\,s^{-1}$. The curve for the inhibition of actin polymerization (Fig. 5 *a*) was generated by repeatedly solving these equations for various concentrations of $[EF1\alpha]_{total}$.

## *Light Scattering*

Samples containing various concentrations of EF1α in PME buffer were rapidly mixed and placed in a fluorimeter (model F2000; Hitachi Sci. In-

strs.), and the amount of scattered light was measured at 600 nm versus time. A tangent drawn to the first 8 s of the reaction was used to indicate the rate of the reaction in arbitrary units.

### *Sedimentation Assay*

Aliquots of spontaneously polymerizing actin or actin polymerized to steady state were spun in a Beckman Airfuge at 28 p.s.i. (140 *g*) for 20 min. The amount of actin remaining in the supernatant was measured by SDS-PAGE densitometry using NIH-Image (version 1.47; written by Wayne Rasband, available via the internet at sippy.nimh.nih.gov). The supernatant amount was compared to an actin standard curve and subtracted from the amount of actin in the initial mixture giving a measure of F-actin. We found it more reproducible to measure the amount of actin in the supernatant rather than the pellet.

### *DNAse Assay*

Conditions for the assay were similar to those described elsewhere (Cooper and Pollard, 1982). DNAse I (Sigma Chemical Co.) was freshly made at 0.1 mg/ml in 50 mM Tris, 100 mM $CaCl_2$, 10 μM PMSF, 20 μM phallacidin (Molecular Probes, Eugene, OR), pH 7.5. Calf thymus DNA (Sigma Chemical Co.) was stored in 100 mM Tris, 4 mM $MgSO_4$, 100 mM KCl, 1.8 mM $CaCl_2$, 0.02% $NaN_3$, pH 7.5, at 40 μg/ml. Aliquots from spontaneously polymerizing samples were mixed with DNAse I and the increase in $OD_{260}$ over time was used to indicate DNAse activity. The amount of G-actin was determined by extrapolation on a standard curve. The standard curve was performed on the same day by incubating serial dilutions of a 2:1 molar ratio of G-actin to EF1α (the same ratio as the assay) in G buffer (2 mM Tris, 0.2 mM ATP, 0.5 mM DTT, 0.2 mM $CaCl_2$, $NaN_3$, pH 8.0). In control experiments, it was found that DNAse activity was equivalent when mixed with either G buffer or PME buffer.

### *Negative Staining*

Polymerizing samples identical to those of Fig. 5 *a* were placed on 300 mesh parlodian grids and immediately stained with 1% uranyl acetate that had been passed through a 0.2 μM Millipore filter and stored on ice. Depolymerizing samples were treated in the same manner; however, to increase the number of filaments, a 10-fold dilution was used to produce a final concentration of 0.8 μM in the presence of 1.5 μM EF1α. Grids were placed under vacuum for at least 20 min before visualization under a transmission electron microscope (model JEM 100 CX II; JEOL USA, Inc., Peabody, MA).

## *Results*

### *EF1α Inhibits the Rate of Actin Polymerization at Molar Ratios Present in the Cytosol*

EF1α constitutes 1–7% of the total cell protein of mitotically active cells (Slobin, 1980; Demma et al., 1990). As EF1α is an actin-binding protein, this abundance suggests that EF1α could influence the assembly properties of actin within cells. Fig. 1 shows that EF1α significantly inhibits actin polymerization at a molar ratio of EF1α/actin (1:2), which was chosen to approximate the ratio of EF1α/G-actin in *Dictyostelium* cytosol (75:180 μm; Hall et al., 1988; Dharmawardhane et al., 1991). Fig. 1, *b* and *c*, shows the effect of EF1α on actin polymerization using high-speed sedimentation and DNAse inhibition. These assays confirm that the fluorescence data presented in Fig. 1 *a* is not an artifact of an interaction between EF1α and the pyrene fluorophore. The small differences between the data of Fig. 1 arise for technical reasons; actin sediments differently when bound to EF1α, whereas DNAse activity had a standard deviation in the time component estimated at 1–2 min. Therefore the differences between the pyrene and DNAse data are not significant.

To confirm that our activity was not due to a contaminant, we assayed the activity of *Dictyostelium* EF1α expressed and purified from *Escherichia coli* as a GST fusion protein (see Liu et al., 1996*b*). This recombinant protein also inhibited actin polymerization, whereas the GST protein alone did not (data not shown).

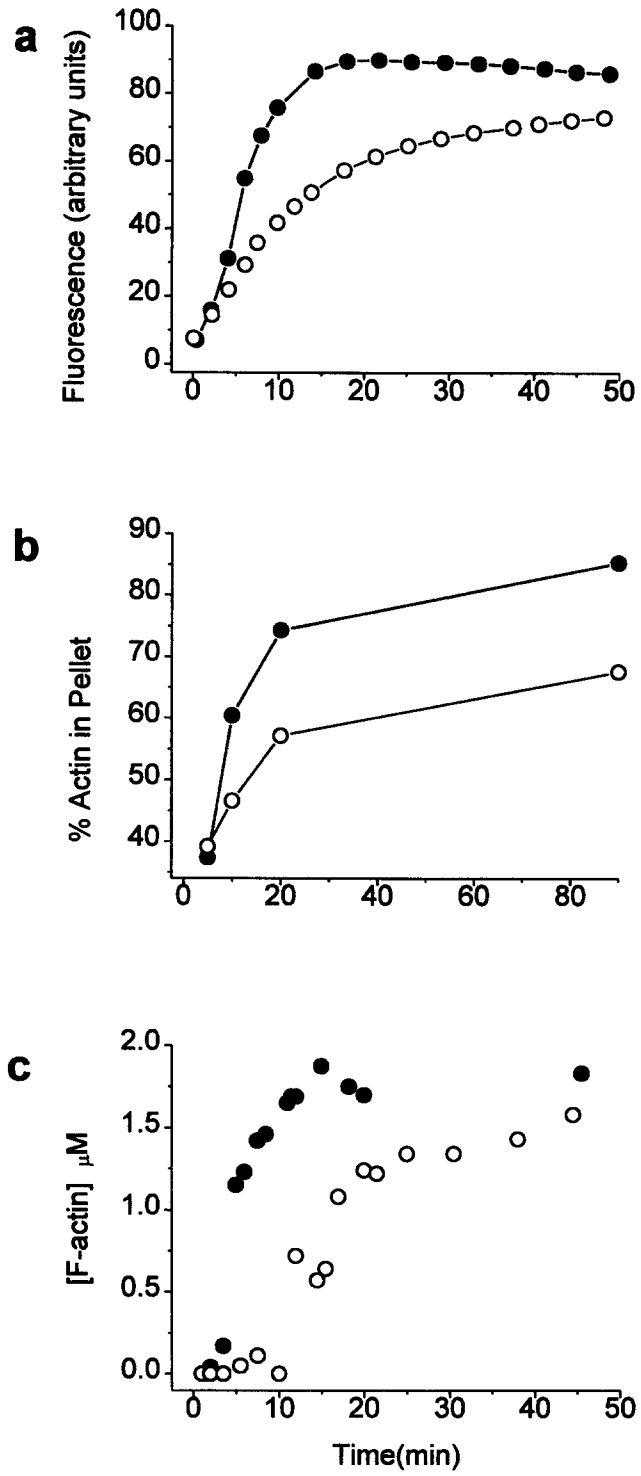


*Figure 1.* Three different methods demonstrate that EF1α alters the actin polymerization reaction. Actin polymerization was initiated by the addition of 2 μM G-actin (from *Dictyostelium*) into PME in the presence (*open circles*) or absence (*filled circles*) of 1 μM EF1α. Polymerization was monitored with: (*a*) pyrene fluorescence, (*b*) sedimentation, and (*c*) DNAse inhibition.

These experiments demonstrate that EF1α can inhibit actin assembly. Furthermore, they demonstrate that the pyrene fluorescence assay provides an accurate measure of actin polymer formation in the presence of EF1α.

Fig. 2 shows the effect of increasing concentrations of native *Dictyostelium* EF1α on actin polymerization. Spontaneous polymerization of actin is characterized by a sigmoidal curve (Fig. 2; 0.0 μM EF1α) where an initial lag is present due to the slow rate of formation of actin nuclei. As seen in Fig. 1, EF1α inhibits actin assembly. However, the presence of high molar ratios of EF1α to actin eliminates the lag phase of polymerization, causing the sigmoidal curve of actin polymerization to become hyperbolic. This suggests that there is an increase in the amount of nuclei at the onset of polymerization in the presence of EF1α. The nucleating effect is concentration dependent in that higher concentrations of EF1α cause greater initial rates of actin polymerization. However, the inhibitory effect of EF1α on actin polymerization still appears to be present at these higher concentrations as seen at time points beyond 450 s when all of the samples containing EF1α have less F-actin compared to the actin alone sample.

### *EF1α Blocks Polymerization at Both the Barbed and Pointed Ends of Actin Filaments*

About 90% of polymer growth occurs at the fast growing, barbed end of actin filaments (Pollard and Cooper, 1986). Because of the dramatic decrease in polymerization rate seen in Fig. 2, it is evident that EF1α can reduce the rate of polymerization from the barbed end. To look at the effect of EF1α at the slow-growing pointed ends of actin filaments, bacterially expressed human gelsolin was used to cap the barbed ends of actin filaments, and these filaments were then used to initiate actin polymerization reactions. Several experiments of this kind are presented in Fig. 3, and these indicate that EF1α also reduces the polymerization rate at the pointed ends of actin filaments. Control experiments showed that inclusion of additional gelsolin had

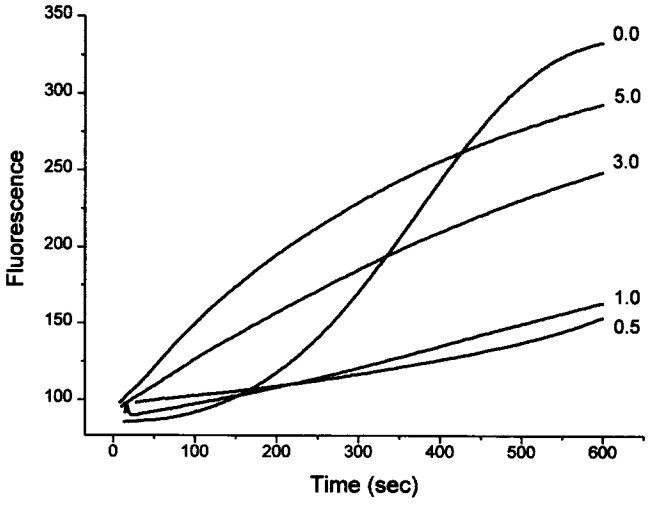


*Figure 2.* The effect of various concentrations of EF1α on actin polymerization. At time zero, 3 μM actin (10% pyrene labeled) was added to a cuvette containing PME buffer and 0–5.0 μM EF1α as indicated at the right of the plots.

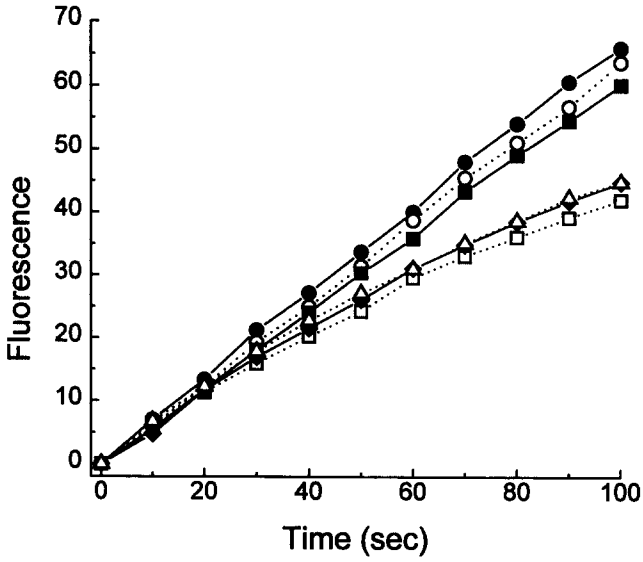


*Figure 3.* The effect of EF1α on gelsolin-capped actin filaments. Gelsolin-capped filaments containing 0.5 μM actin and 0.02 μM gelsolin were used to initiate the polymerization of 1.5 μM G-actin in PME buffer and various concentrations of EF1α. Polymerization curves are shown for six different concentrations of EF1α: (●) 0.0 μM, (○) 0.1 μM, (■) 0.2 μM, (□) 0.5, (◆) 1.0 μM, (△) 2.0 μM.

no effect on actin polymerization, indicating that free barbed ends were not generated during the experiment (not shown). Unlike the effects of EF1α on actin polymerization in the absence of gelsolin, the inhibition of the rate of actin polymerization from gelsolin-capped filaments is apparent only after the reaction has proceeded for 20–30 s. This delay was not dependent on the concentration of EF1α and therefore does not appear to be a binding step of EF1α. As for polymerization in the absence of gelsolin, the degree of polymerization inhibition is concentration dependent. Maximal divergence from the control curve occurs at 0.5 μM EF1α, the same concentration responsible for maximal inhibition of polymerization in the absence of gelsolin (see Fig. 5 *a*). We also observed a greater divergence in the curves when the gelsolin/actin ratio was increased, that is, when the filaments were shorter and the overall reaction rate (in the control) was faster (data not shown).

### *Monomer Binding*

Binding of EF1α to actin monomer has been observed previously (Dharmawardhane et al., 1991); however, we needed to know if EF1α was binding to actin monomer under conditions where it inhibits actin polymerization. We used the method of Lee and Pollard (1988) to measure binding to G-actin in solution (Fig. 4). EF1α causes an increase in G-actin pyrene fluorescence as measured at excitation 344 nm and emission 386 nm, and this increase in fluorescence conforms to a parabolic curve when the concentration of EF1α is varied and corresponds to monomer binding. The experiment was repeated using EF1α bound to GTP and GDP, and these data were fit to bimolecular binding isotherms resulting in the following equilibrium dissociation constants: 1.4, 0.7, and 3.9 μM for EF1α

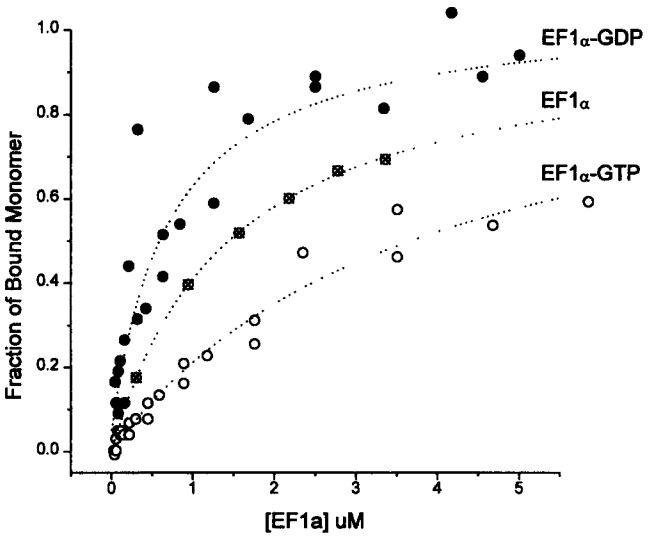


*Figure 4.* Binding of actin monomer by EF1α. The fluorescence of actin monomer was recorded in the presence of various concentrations of EF1α. This data was plotted as the fraction of actin monomer bound using a bimolecular binding isotherm resulting in $K_d$s of 0.7, 3.9, and 1.4 μM for EF1α in three different states: EF1α bound to GDP, GTP, and EF1α as freshly isolated, respectively.

(freshly isolated), EF1α-GDP, and EF1α-GTP, respectively. These results suggest that freshly isolated EF1α is a mixture of GTP and GDP forms.

To rule out the possibility that the fluorescence increase is due to polymerization of G-actin, we used a concentration of G-actin (0.05 μM) well below the critical concentration for polymerization. Additionally, the fluorescent signal was calibrated in terms of actin polymer fluorescence, and finally the binding experiment was repeated in the presence of DNAse. The fluorescence calibration demonstrated that the maximal fluorescence signal increase was equivalent to about 3 nM F-actin, much less than expected if the actin were polymerizing. Furthermore, DNAse did not prevent the increase in fluorescence seen in the presence of EF1α, demonstrating that changes in fluorescence were not due to actin polymerization. Although we did not pursue these competition experiments further, this result suggests that EF1α and DNAse are binding to different surfaces of the actin monomer.

### *Quantitative Analysis of the Inhibition of Actin Polymerization by EF1α*

To quantitate the effect of EF1α on rapidly polymerizing actin, we initiated actin polymerization from preformed, sheared actin filaments. Fig. 5 *a* shows a plot of the percent inhibition of the initial rate of actin polymerization versus the concentration of EF1α. EF1α significantly inhibits the initial rate of actin polymerization at substoichiometric levels to G-actin. Using the $K_d$ derived from Fig. 4, we plotted the expected amount of inhibition if EF1α were sequestering actin monomers (*open squares*). Furthermore we plotted the result expected if EF1α were sequestering two actin monomers for every one EF1α molecule (*crossed squares*). Neither of these mechanisms could account for the extent of inhibition seen at low concentrations of EF1α. We also plotted the best fit to the observed data if EF1α were inhibiting actin polymerization by capping both ends of the actin filament (Fig. 5 *a*, *solid line*). This curve is very similar to what would be observed for a barbed-end capping protein except that the maximal percent inhibition of a barbed-end capping protein would be ~90% and that of a double-end capping protein would be 100%. Note that the double-end capping model shows better agreement with the observed data than the monomer sequestering models. However, the double-end capping model cannot account for the 80% inhibition seen at 0.5 μM EF1α and still account for the 20–30% inhibition seen at 0.25 μM EF1α, no matter what the affinity of the capping protein for the ends of the filament (the curve shown here is the best fit, which gave a $K_d$ of 0.34 μM). That is, the shape of the curve of this model is distinctly different from that of the observed data. In addition, the capping model plateaus at 100% inhibition, whereas the observed data plateaus at 78% inhibition. Attempts to model the observed data with a capping protein that has different affinities for the barbed and pointed ends showed little improvement over the capping model in Fig. 5 as these models saturate at 100% inhibition of actin polymerization.

In several sets of experiments performed with a lower number concentration of actin filament ends compared to Fig. 5 *a*, the extent of the inhibition of the initial rate of polymerization reached a maximum at 60% or less (see Fig. 8). Therefore, this quantitative analysis suggests that EF1α does not inhibit actin polymerization through capping of the filament ends. However, because EF1α can alter the rates of actin polymerization at substoichiometric molar ratios to G-actin (for example in Fig. 5 *a*, 0.44 μM EF1α inhibited the rate of 1.5 μM G-actin by 75%), the actual mechanism likely involves the blockage or loss of filament ends rather than some effect on actin monomer.

We generated a curve for the inhibition of actin polymerization by EF1α according to a bundling mechanism (Fig. 5 *a*, *open circles*). This mechanism assumes that as filaments are cross-linked and enter a bundle their ends become annealed and/or sterically buried from solution.

Intuitively, the mechanism explains the data in Fig. 5 *a* as the maximal percent inhibition of actin polymerization (Fig. 5 *a*) is determined by the rate at which the filament ends are annealed/buried from solution, i.e., it is determined by the loss-of-filament-end rate constant and the concentration of filament ends (see Materials and Methods). Therefore, the percent inhibition is expected to saturate at a value that is below 100% and dependent on the initial concentration of filament ends. On the other hand, the cooperative appearance of Fig. 5 *a* is explained because a "critical fraction" of bound EF1α is required for actin bundling. This minimal ratio was measured at 13 F-actin subunits per 4 EF1α-bound F-actin subunits (Fig. 5 *b*) and is therefore comparable to a hill coefficient of cooperativity of 13/4 = 3.25.

A value of 250 $\mu M^{-1}$ $s^{-1}$ for the rate constant for the loss of filament ends was found by fitting the model to the observed data, whereas the amount of F-actin that has attained the critical fraction of bound EF1α was found by measuring the critical molar ratio required for bundling (Fig. 5 *b*) and using the $K_d$ for the binding of EF1α to F-actin

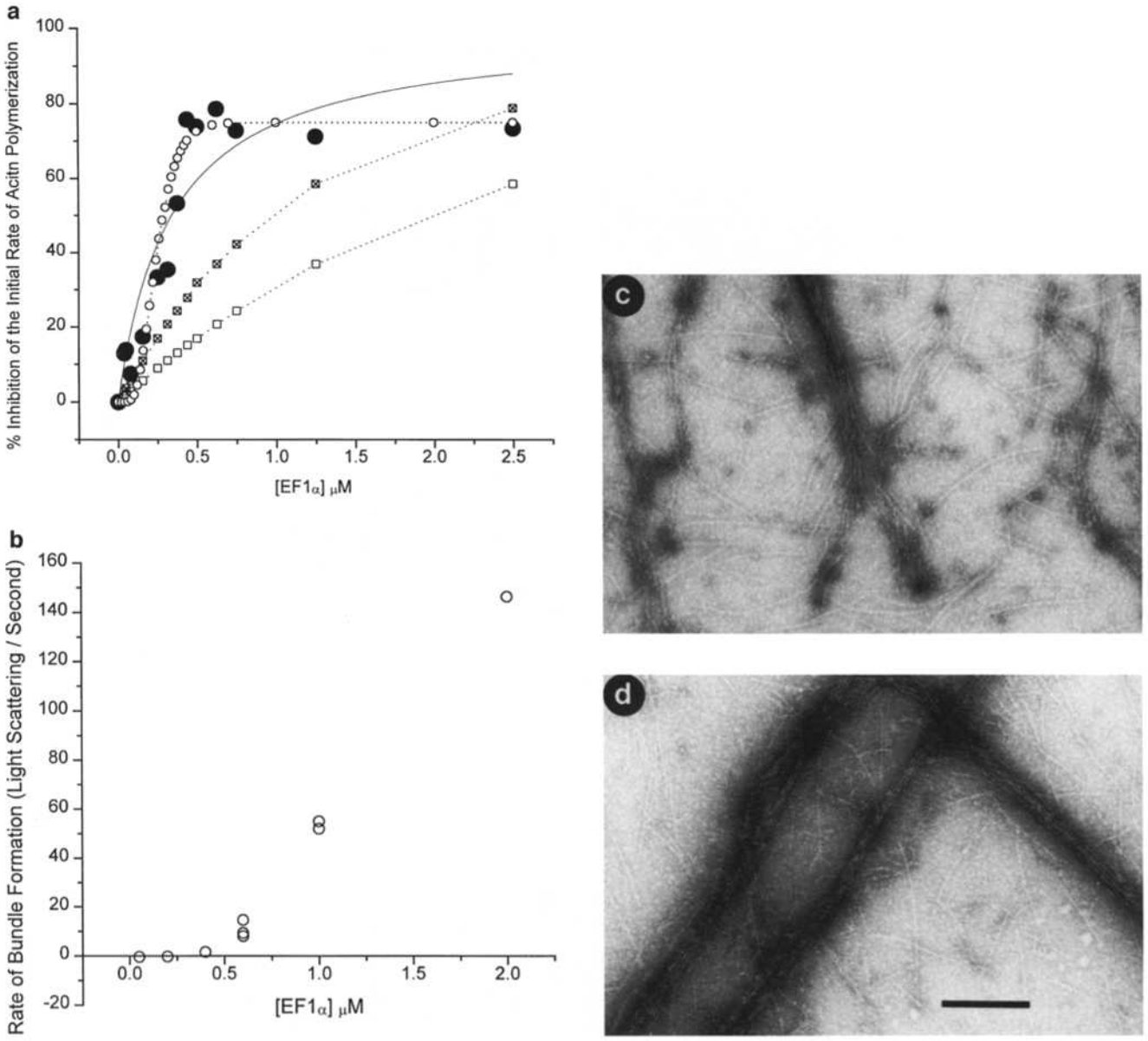


*Figure 5.* Quantitative analysis of the inhibition of actin polymerization by EF1α. (*a*) The filled circles show the observed inhibition of actin polymerization of 1.5 μM G-actin by EF1α in the presence of 0.5 μM F-actin seeds. Also shown are four possible mechanisms for this inhibition: monomer binding (*open squares*), dimer binding (*crossed squares*), capping (*solid line*), and bundling (*open circles*). The affinity constant for the monomer-binding mechanism (1.4 μM) comes from Fig. 4, the capping mechanism is a chi-square best fit to the data (resulting $K_d$ = 0.34 μM), and the affinity constant for the bundling mechanism (0.2 μM) comes from Edmonds et al. (1995). (*b*) The effect of EF1α on the rate of bundle formation; the minimal concentration of EF1α required for bundle formation was used in generating the bundling mechanism (see Materials and Methods). (*c* and *d*) Electron micrographs of polymerizing samples containing 0.5 μM EF1α 20 s (*c*) and 60 s (*d*) after addition of seeds. Note the presence of bundles that become more ordered by 60 s. Bar, 0.25 μm.

(Edmonds et al., 1995). A statistical distribution of the F-actin population was also incorporated into this model (see Materials and Methods). The large value of the rate constant for the loss of filament ends arises mathematically because the rate constant is second order to the number of filament ends, which are at low concentration (0.6 nM). However, bundling of actin filaments by EF1α causes the filaments to cross-link and align, and therefore the interaction of the filament ends is not dependent on their diffusion through solution.

Samples identical to those of Fig. 5 *a* were negatively stained and viewed by electron microscopy and photographs of these results are shown in Fig. 5, *c* and *d*. By 20 s after the addition of filament seeds to samples containing G-actin and EF1α, the samples already contained numerous bundles with 2–6 actin filaments. In addition, filaments that are not yet bundled often appear ordered into parallel arrays, indicating that EF1α was affecting their organization. In contrast, the control experiments showed a random ordering of single actin filaments. This demonstrates that EF1α is cross-linking F-actin at early times during these polymerization experiments and suggests that fila-

ments within the bundles contribute to polymerization at these early times.

### *The Effect of EF1α on F-Actin at Steady State*

When actin is polymerized to apparent equilibrium (steady state), a small portion of the actin will remain unpolymerized (the critical concentration). Monomer-sequestering proteins will increase the apparent critical concentration by binding actin monomer in a way that is competitive with polymerization. Barbed end capping proteins will also increase the apparent critical concentration by shifting the critical concentration from that of the barbed end (~0.2 μM) to that of the pointed end (~0.6 μM). To determine if EF1α behaves like either of these classes of proteins, actin was polymerized to steady state in the presence or absence of EF1α, and the actin critical concentration was measured by pyrene fluorescence and high-speed sedimentation. The results shown in Fig. 6 indicate that EF1α decreases the actin critical concentration in a manner that is dependent on the concentration of EF1α. For comparison, gelsolin was included in these assays (*open circles*), and as expected, gelsolin caused the actin critical concentration to increase to a value near 0.6 μM. The effect of EF1α on actin critical concentration was also measured on gelsolin-capped filaments (Fig. 6 *c*). Again, EF1α was seen to decrease the apparent critical concentration (indicated by an increase in fluorescence). This indicates that EF1α behaves neither like a monomer-sequestering protein nor a barbed end capping protein. Curves were fit to the data of Fig. 6 (*dotted lines*) and resulted in $K_d$s for EF1α of 0.14 (*a*), 0.4 (*b*), and 0.92 μM (*c*). $K_d$s for gelsolin were 0.3 (*a*) and 0.5 nM (*b*). These curve fits are considered approximations due to the level of noise in the assay and their unspecified (free floating) maxima and minima but are consistent with the $K_d$ measured for the binding of EF1α to F-actin under similar buffer conditions (Edmonds et al., 1995).

### *The Effect of EF1α on Actin Depolymerization*

Since EF1α inhibits actin polymerization but also decreases the actin critical concentration (i.e., drives monomer into filament), we expected that EF1α would also inhibit actin depolymerization. A representative depolymerization curve (Fig. 7 *a*, *inset*) demonstrates that EF1α inhibits the rate of depolymerization. The data were plotted as the percent inhibition of initial actin depolymerization rate versus the concentration of EF1α (Fig. 7 *a*, *filled circles*). The electron micrographs shown in Fig. 7 *b* demonstrate that actin-EF1α bundles are formed during the 3-min incubation period before depolymerization and that these bundles persist during depolymerization and are presumably the species that is resistant to depolymerization.

### *The Effect of pH on the Interaction between EF1α and Actin*

Measurements of the pH of *Dictyostelium* cytoplasm indicate a broad range of values between 6.0 and 8.2 with a median between 6.8 and 7.2 (Satre et al., 1986; Furukawa et al., 1988, 1990). Resting pH increases 0.2–0.4 U by 90 s after stimulation with cyclic AMP (Aerts et al., 1987; Van

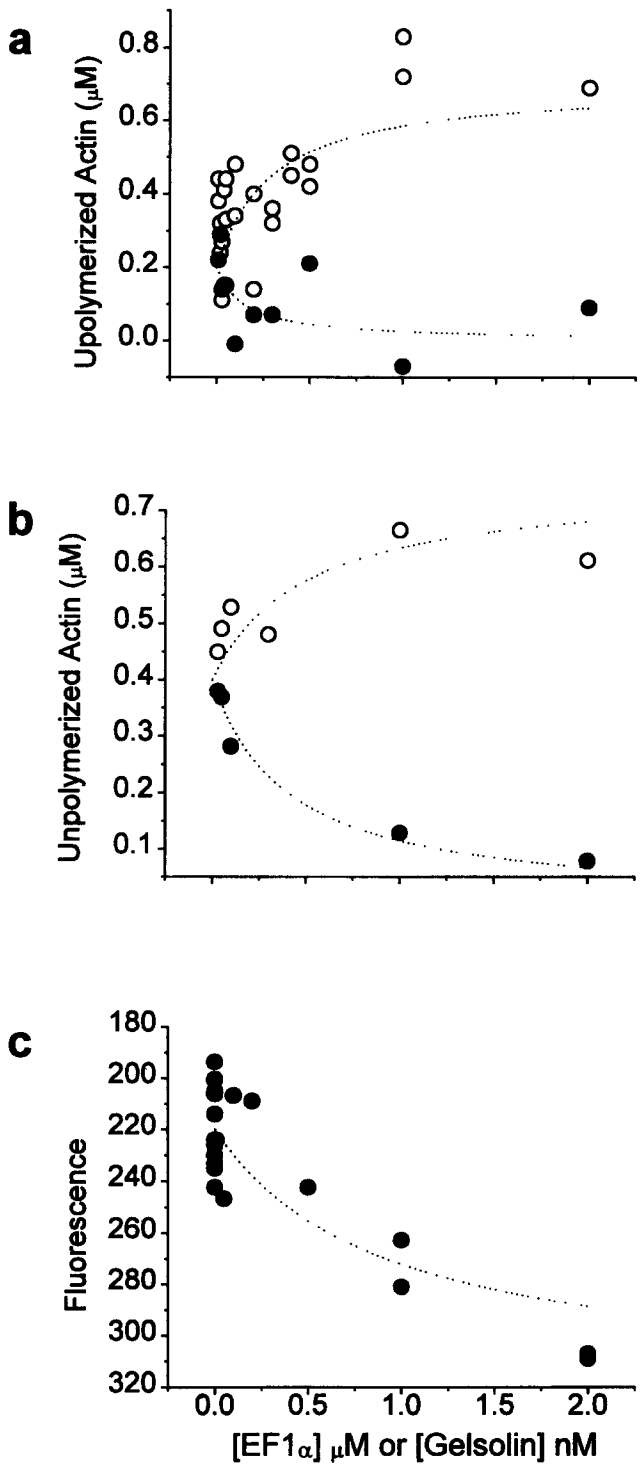


*Figure 6.* The effect of EF1α on the F-actin critical concentration. Actin was polymerized to steady state (>18 h) in the presence of 0.0–2 μM EF1α (●), or 0.0–2.0 nM Gelsolin (○), or 20 nM gelsolin and 0.0–2 μM EF1α (●, *c*). The remaining unpolymerized actin (the critical concentration) from uncapped actin filaments was measured using calibrated pyrene fluorescence (*a*), sedimentation (*b*), or uncalibrated pyrene fluorescence (*c*).

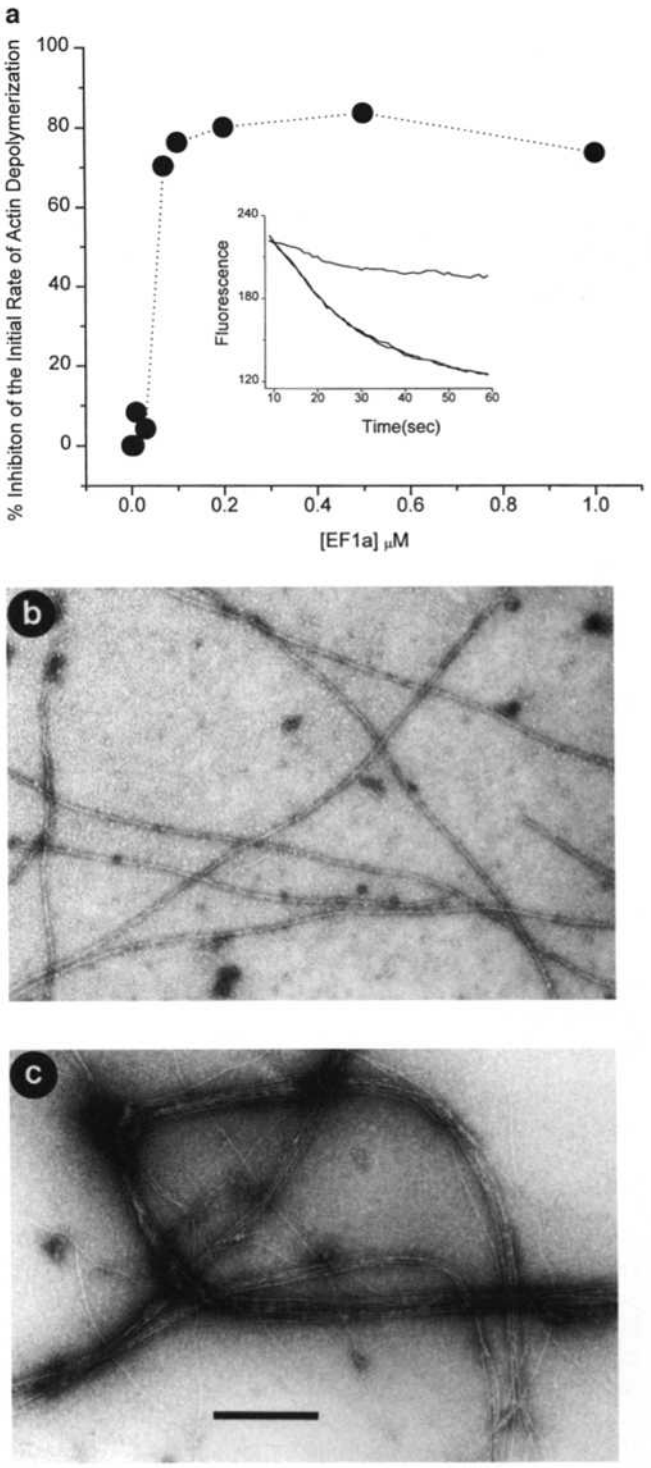


*Figure 7.* The inhibition of the initial rate of actin depolymerization by EF1α. (*a*) Actin was depolymerized to a final concentration of 0.03 μM in the presence and absence of EF1α and the observed percent inhibition of the initial rate of depolymerization was plotted versus the EF1α concentration (*filled circles*) in the same manner as for Fig. 5. (*Inset*) Examples of F-actin depolymerization. The lower curves show two examples of actin alone while the upper curve shows actin plus 0.07 μM EF1α. (*Bottom*) Electron micrographs of actin depolymerizing alone (*b*), and in the presence of EF1α (*c*). Bar, 0.25 μm.

Duijn and Inouye, 1991), and cyclic AMP causes a redistribution of F-actin and EF1α within this time frame (Dharmawardhane et al., 1991; Okazaki and Yumura, 1995). These observations and the observation that protein synthesis can be regulated by pH (Aerts et al., 1985; Liu et al., 1996*a*) have led us to investigate the effects of pH on the inhibition of actin polymerization by EF1α. It was determined that high pH inhibits cross-linking of actin filaments with a transition from cross-linking to single filament binding occurring at pH 7.0 (Edmonds et al., 1995).

To determine if pH affects the inhibition of actin polymerization by EF1α, actin was polymerized in the presence or absence of EF1α over the range of pH values present in *Dictyostelium* cytoplasm. The data presented in Fig. 8 show that the inhibition of actin polymerization by EF1α is affected by pH in the same manner as the bundling of F-actin by EF1α. At low pH, the inhibitory activity is on while at high pH this activity is off. Accordingly, the data has been fit to sigmoidal curves to indicate the transition from the on to off state, which occurs around pH 7.0.

### *The Effect of Aminoacyl-tRNA*

During protein translation, EF1α binds aminoacyl-tRNA and this complex interacts with the active ribosome. In vitro when EF1α binds to GTP, the GTP–EF1α complex will bind to aminoacyl-tRNA to form a stable EF1α-GTP–aminoacyl-tRNA ternary complex. Liu et al. (1996*b*) have shown that ternary complex formation inhibits EF1α's F-actin-bundling activity, suggesting that the aminoacyl-tRNA–binding site overlaps with at least one of the F-actin–binding sites on EF1α. Therefore, we measured the effect of aminoacyl-tRNA bound EF1α on actin polymerization. The results (Fig. 9) show that both EF1α and EF1α-GTP reduce the rate of actin polymerization as compared to actin alone. However, when phe-tRNA is allowed to bind

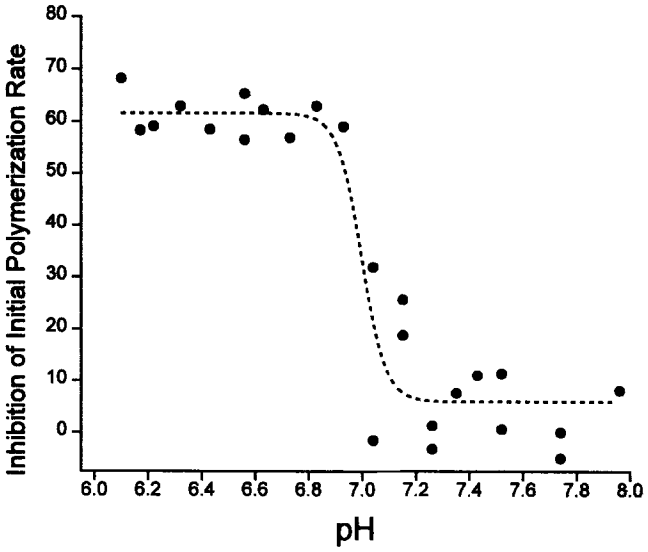


*Figure 8.* The effect of pH on the inhibition of actin polymerization by EF1α. Actin (1.5 μM G-actin, 0.5 μM F-actin seeds) was polymerized in the presence and absence of 0.5 μM EF1α, and the inhibition of actin polymerization was calculated as in Fig. 5 *a*. The data were curve fit to illustrate the transitional effect of EF1α on actin as the pH is raised.

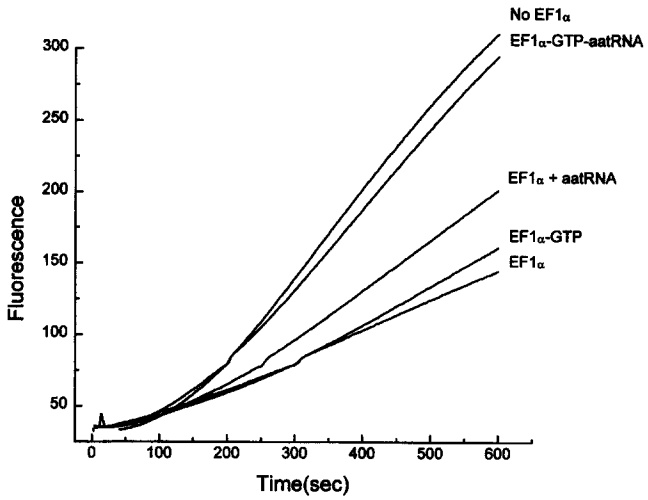


*Figure 9.* The effect of aminoacyl-tRNA binding on the ability of EF1α to alter actin polymerization. At time zero, G-actin was added to PME in the presence of no EF1α, freshly isolated EF1α, EF1α and aminoacyl-tRNA, EF1α-GTP, and EF1α-GTP–aminoacyl tRNA, as indicated. The concentrations were 3 μM actin, 1 μM EF1α, and 0.8 μM aminoacyl-tRNA.

GTP-EF1α and this complex is added to the actin polymerization assay, a restoration of normal rate of actin polymerization is observed. When phe-tRNA was included with EF1α in the absence of GTP, a small reduction of the inhibition of actin polymerization was still observed, suggesting that some of the EF1α as purified is a mixture of GTP and GDP forms and that the GTP form is aminoacyl-tRNA binding–competent in the absence of exogenous GTP.

## Discussion

### The Many Roles of EF1α

Although EF1α has been described as a translation factor for many years, increasing evidence suggests that EF1α may have other roles within the cell. EF1α binds and severs microtubules (Durso et al., 1994; Shiina et al., 1994). Other reports indicate that EF1α can activate phosphatidylinositol 4-kinase (Yang et al., 1993) and bind calmodulin (Kaur and Ruben, 1994). The association of EF1α with actin has been demonstrated by several labs both in vivo and in vitro (Dharmawardhane et al., 1991; Bassell et al., 1994*a*; Bektas et al., 1994; Collings et al., 1994; Edmonds et al., 1995, 1996); however, the activities of EF1α with respect to actin have not been fully documented.

Perhaps it should not be surprising that EF1α possesses these other activities as it has been estimated that EF1α is 14 times more abundant than the amount of specific aminoacyl-tRNA and up to 35 times more abundant than ribosomes within eukaryotic cells (Slobin, 1980). We presume that the abundance of EF1α means that binding of even a fraction of EF1α to F-actin would have significant consequences for cytoskeletal function within a cell. The role of actin and microtubules in the transport, anchorage, and regulation of the protein synthetic machinery has become an area of vigorous research, and it appears that the compartmentalization of this nondiffusible machinery may be key for its proper functioning (Bassell et al., 1994*b*). The ability of EF1α to sever microtubules and, as presented in this report, the ability of EF1α to alter the rates of actin polymerization suggests that EF1α may have an important role in establishing a cytoskeletal topography which is required for the spatial control of protein synthesis (Shiina et al., 1994; Condeelis, 1995).

### EF1α's Effects on Actin Dynamics Cannot Be Explained by Monomer Binding or Filament Capping

As demonstrated here, purified EF1α decreases the rates of actin polymerization and depolymerization in a concentration-dependent fashion. EF1α is an actin filament–binding and –bundling protein. However, it is also reported to bind actin monomer cross-linked to Sepharose beads (Dharmawardhane et al., 1991). None of our data indicates that the binding of EF1α to G-actin is inhibitory towards actin polymerization. Inhibition of actin polymerization occurs at EF1α concentrations that are substoichiometric to G-actin (Figs. 2 and 5 *a*). Using the $K_d$ derived from monomer binding experiments (1.4 μM, Fig. 4), we could not account for the extent of inhibition of actin polymerization even when we assumed each EF1α bound two actin monomers, and especially if the amount of EF1α that is expected to be bound to F-actin is accounted for (not shown). Experiments conducted using native gel electrophoresis also failed to show significant EF1α–actin monomer interaction at concentrations below 1 μM (data not shown). Furthermore, the observed data of Fig. 5 *a* appears cooperative, comparable to a binding curve with a hill coefficient of >3. This means that as a monomer-sequestering protein, EF1α would have to bind >3 actin monomers to explain the appearance of the data of Fig. 5 *a*. In addition, EF1α caused the actin critical concentration to decrease rather than increase, indicating that EF1α is not involved in sequestering of actin monomers.

The inhibition of actin polymerization and depolymerization by EF1α appears qualitatively similar to that of barbed end capping proteins (compare our Fig. 2 to Fig. 1 of Cooper and Pollard, 1985). However, the affinity of EF1α for actin filaments is much weaker than the affinity of well-known capping proteins such as gelsolin ($K_d$ < 0.1 nM; Lo et al., 1994; 0.3–0.5 nM in this report, Fig. 7) and capZ ($K_d$ ~ 0.5 nM; Caldwell et al., 1989). Furthermore, Fig. 3 demonstrates that EF1α can inhibit actin polymerization from gelsolin-capped actin filaments. This inhibition is concentration dependent showing a maximal inhibition at 0.5 μM EF1α, the same concentration for maximal inhibition as seen in the absence of gelsolin. Since polymerization rates from uncapped filaments can be inhibited by 78% (Fig. 5 *a*), the fast-growing ends must also be inhibited, and hence EF1α can block polymerization from both ends of an actin filament. Therefore, EF1α does not inhibit actin polymerization by selectively capping either end of the actin filament. Additionally, modeling the data of Fig. 5 *a* using a capping mechanism did not generate curves that fit the observed data regardless of whether we took into account the amount of EF1α that would be bound to the sides of actin filaments (not shown).

EF1α also decreases the actin critical concentration (Fig. 6), a result inconsistent with filament end capping.

For comparison, gelsolin was included in these experiments, which caused the actin critical concentration to increase towards that of the pointed end as previously reported (Selve and Wegner, 1986). The effect of EF1α on the critical concentration was furthermore not dependent on free barbed ends since gelsolin-capped filaments also had a lower critical concentration in the presence of EF1α (Fig. 6 *c*).

### *Inhibition of Actin Polymerization by EF1α Requires Filament Bundling*

Addition of EF1α to a solution of actin monomers or filaments results in rapid bundle formation. At the earliest times assayed, filaments were gathered into bundles under the polymerization and depolymerization conditions used in this study. Bundling of filaments would lead to steric blockade of monomer addition to filament ends as the ends become buried in the growing bundle and/or become annealed because of their juxtapositioning in the bundle.

In Fig. 5 *a*, we demonstrate that a mechanism based on the bundling activity of EF1α can account for the observed effect of EF1α on actin polymerization. Consistent with this model is the observation that agents that inhibit bundling by EF1α release the EF1α-mediated inhibition of actin polymerization. For example, increases in pH over the physiological range have been shown to convert the actin-binding activity of EF1α from cross-linking to single filament binding (Edmonds et al., 1996). This is consistent with the identification of two actin-binding sites in EF1α with different pH sensitivities for actin binding (Liu et al., 1996*b*) and explains the association of EF1α with single actin filaments, filament branch points, and filament bundles in situ (Bassell et al., 1994; Liu et al., 1996*a*). Transition of EF1α from cross-linking to monovalent filament binding occurs at the same pH as the loss of EF1α-mediated inhibition of actin polymerization (Fig. 8 and Edmonds et al., 1995), suggesting a causative relationship between bundling and inhibition of polymerization. Furthermore, the binding of EF1α to aminoacyl-tRNA has been shown to inhibit the bundling activity of EF1α (Liu et al., 1996*b*). As seen in Fig. 9, the addition of aminoacyl-tRNA to GTP-EF1α dramatically reduced the inhibition of actin polymerization by EF1α, again suggesting a causative relationship between EF1α-mediated bundling and the inhibition of actin polymerization.

The cross-linking of actin filaments by EF1α is expected to slow actin depolymerization because more molecular bonds must be broken to release an actin subunit from a filament, and this was observed (Fig. 7). The reduction in the rate of actin depolymerization is also expected to increase the amount of F-actin observed at steady state (i.e., reduce the actin critical concentration), and this was observed (Fig. 6). In addition, since filament ends within a bundle are not solution accessible and/or are annealed, it is also expected to take longer for the actin polymerization reaction to reach equilibrium, which we have also observed (Fig. 2, and data not shown).

The ability of EF1α to bind actin monomer and short growing filaments also accounts for the nucleation activity of EF1α since the *EF1α · F-actin* complex is resistant to depolymerization. At low concentrations, EF1α binds and stabilizes F-actin (Fig. 7) and, as the monomer binding experiment of Fig. 4 shows, above 1 μM EF1α binds a significant amount of actin monomer. This binding of actin monomer may cause the stabilization of actin oligomers that would act as actin nuclei and stimulate the initial actin polymerization rate as seen in Fig. 2. Although the actin nuclei are initially capable of actin polymerization, they are also susceptible to end-burying/annealing as filaments elongate and F-actin bundles form. Therefore, the bundling mechanism is consistent with and explains all of the kinetic and steady-state effects of EF1α on actin polymerization and depolymerization.

### *Bundling Proteins and Actin Polymerization*

There are many examples of proteins that bundle actin filaments as well as affect actin polymerization. There is not room here for a full discussion of this topic. However, we will mention a couple of relevant examples. Talin, an actin-binding protein present in focal contacts, is a pH-sensitive actin-bundling protein that can also nucleate actin polymerization (Goldman et al., 1994; Zhang et al., 1996). Goldman et al. (1994) demonstrate, as we have shown here for EF1α, that the nucleating effect of talin is only apparent at the onset of a polymerization experiment and that at later times in the experiment the polymerization rate may be slower in the presence of talin than in its absence. For an explanation of this behavior, these authors site the ability of talin to rapidly reduce the length distribution of actin filaments, which corresponds to actin filament nucleation, and subsequently anneal the actin filament/talin protein polymer network (Ruddies et al., 1993), which corresponds to a reduction in the actin polymerization rate.

Another group of proteins, the synapsins, are neuronal phosphoproteins localized to the cytoplasmic surfaces of synaptic vesicles. Synapsins are believed to regulate neurotransmitter release by cross-linking vesicles into the actin cytoskeleton (Greengard et al., 1993). Synapsins can bundle actin filaments and nucleate actin polymerization. Furthermore, unphosphorylated synapsin I inhibits actin depolymerization, increases the steady-state levels of F-actin relative to G-actin, decreases the apparent rate constant of actin polymerization, and causes actin to polymerize under nonpolymerizing salt concentrations (a property also observed with EF1α; data not shown). In other words, qualitatively, synapsin I displays nearly all of the properties toward actin polymerization that we have here demonstrated for EF1α.

Fesce et al. (1992) have analyzed the effects of synapsin I on actin polymerization by fitting mathematical models to curves of actin polymerization versus time as well as to curves of the derivative of these curves (the rate of loss of actin monomer). This approach led Fesce et al. to conclude that synapsin I nucleates actin polymerization by binding 4 actin monomers and that polymerization from these nuclei occurs at a slow rate compared to actin alone. Assuming that synapsin I and EF1α affect actin polymerization by a similar mechanism, we propose that the reduction in polymerization rate by these proteins is due to burying/annealing of filament ends as opposed to an effect on actin monomer. As noted, we have found that the dif-

ference between the rate of actin polymerization in the presence and absence of EF1α is greater when the initial concentration of ends (the number concentration) is greater, indicating that the effect is dependent (in a non–first-order manner) on the concentration of preexisting filament ends. It is interesting that both groups came up with a mechanism that requires that three to four actin subunits are affected by one subunit of the protein of interest.

Shiina et al. (1994) have detected a microtubule-severing activity of EF1α. We did not detect severing of actin filaments by EF1α; instead, EF1α stabilized actin filaments from depolymerization. It is possible that conditions may be discovered that activate an actin-severing activity of EF1α. In addition, it is also possible that the nucleating activity of EF1α could effectively decrease the filament length distribution, as has been postulated in the case of talin, which lowers actin filament length distribution (Kaufmann et al., 1991; Goldmann et al., 1994), giving the impression of severing by redistributing actin monomer onto numerous nuclei stabilized by EF1α.

## *EF1α, Actin Binding, and Translation*

EF1α binds to G- and F-actin and inhibits actin polymerization in both the GTP-bound and freshly isolated forms (Dharmawhardhane et al., 1991; Figs. 4 and 9, this report). In the GTP-bound form, EF1α also binds to aminoacyl tRNA at sites that overlap with the F-actin–binding sites (Liu et al., 1996*b*). In the absence of aminoacyl-tRNA, EF1α will interact with F-actin to form cross-linked filaments that polymerize and depolymerize slowly and that exhibit a decreased critical concentration at steady state. These results predict that in vivo, filaments that are observed to interact with EF1α (Edmonds et al., 1995, 1996; Liu et al., 1996*b*) represent a less dynamic subset of filaments with polymerization properties different from those filaments not bound to EF1α. Upon binding of aminoacyl-tRNA to the GTP-bound form of EF1α to make the ternary complex, a reaction that appears to involve the direct interaction between EF1α and aminoacyl tRNA-synthetase in vivo (Stapulionis and Deutscher, 1995), EF1α would be released from its cross-linking interaction with actin filaments, thereby supplying a high local concentration of ternary complex for polypeptide elongation. Small increases in pH around 7.0 bias the binding of EF1α to aminoacyl-tRNA over F-actin (Liu et al., 1996*b*) and in vivo would regulate the availability of EF1α for translation and its binding to the actin cytoskeleton. This is consistent with the observation that small increases in pH are correlated with increases in protein synthesis in a variety of cell types (Liu et al., 1996*a*).

Coincidentally, filaments released from binding to EF1α by aminoacyl-tRNA would return to a more dynamic state, undergoing more rapid polymerization, depolymerization, and/or physical rearrangements. This is consistent with several observations that small increases in pH are correlated with changes in vivo in the localization of EF1α with F-actin, reorganization of the actin cytoskeleton, and increases in cell locomotion (Aerts et al., 1987; Dharmawardhane et al., 1991; Van Duijn and Inouye, 1991; Edmonds et al., 1995). Therefore, the ability of EF1α to influence the assembly and structure of the actin cytoskeleton in vivo could be a key step regulating the transport, anchorage, and translation of mRNA on actin filaments.

We acknowledge the Analytical Imaging Facility for help with electron microscopy.

This work was supported by National Institutes of Health grant GM25813 and training grant 5T32 CA09475-10.

Received for publication 17 June 1996 and in revised form 10 September 1996.

### *References*

Aerts, R.J., A.J. Durston, and W.H. Moolenaar. 1985. Cytoplasmic pH and the regulation of the *Dictyostelium* cell cycle. *Cell.* 43:853–857.

Aerts, R.J., R.J.W. De Wit, and M.M. Van Lookeren Campagne. 1987. Cyclic AMP induces a transient alkalinization in *Dictyostelium. FEBS Lett.* 220: 366–370.

Bagshaw, C.R., and D.A. Harris. 1987. Measurement of ligand binding to proteins. *In* Spectrophotometry & Spectrofluorimetry. A Practical Approach Series. D.A. Harris and C.C. Bashford, editors. IRS Press, Oxford. 91–113.

Bassell, G.J., C.M. Powers, K.L. Taneja, and R.H. Singer. 1994*a*. Single mRNAs visualized by ultrastructural *in situ* hybridization are principally localized at actin filament intersections in fibroblasts. *J. Cell Biol.* 126:863–876.

Bassell, G.J., K.L. Taneja, E.H. Kislauskis, C.L. Sundell, C.M. Powers, A. Ross, and R.H. Singer. 1994*b*. Actin filaments and the spatial positioning of mRNAs. *Adv. Exp. Med. Biol.* 358:183–189.

Bektas, M., R. Nurten, Z. Gurel, Z. Sayers, and E. Bermek. 1994. Interactions of eukaryotic elongation factor 2 with actin: a possible link between protein synthetic machinery and the cytoskeleton. *FEBS Lett.* 356:89–93.

Bresnick, A.R., and J. Condeelis. 1991. Isolation of actin-binding proteins from *Dictyostelium discoideum. Methods Enzymol.* 85:70–83.

Caldwell, J.E., S.G. Heiss, V. Mermall, and J.A. Cooper. 1989. Effects of capz, an actin capping protein of muscle, on the polymerization of actin. *Biochemistry.* 28:8506–8514.

Collings, D.A., G.O. Wasteneys, M. Miyazaki, and R.E. Williamson. 1994. Elongation Factor 1 α is a component of the subcortical actin bundles of characean algae. *Cell Biol. Int.* 18:1019–1024.

Condeelis, J. 1995. Elongation factor 1 α and the regulation of cytoskeletal dynamics, mRNA sorting and growth control. *Trends Biochem. Sci.* 233:169–215.

Condeelis, J., and N. Vahey. 1982. A calcium and pH regulated protein from *Dictyostelium discoideum* that crosslinks actin filaments. *J. Cell Biol.* 94:466–471.

Cooper, J.A., and T.D. Pollard. 1982. Methods to measure actin polymerization. *Methods Enzymol.* 85:181–211.

Cooper J.A., and T.D. Pollard. 1985. Effect of capping protein on the kinetics of actin polymerization. *Biochemistry.* 24:793–799.

Crechet, J.B., and A. Parmeggiani. 1986. Characterization of the elongation factors from calf brain 3. Properties of the GTPase activity of EF-1α and mode of action of kirromycin. *Eur. J. Biochem.* 161:655–660.

Demma, M., V.W. Warren, R. Hock, S. Dharmawardhane, and J. Condeelis. 1990. Isolation of an abundant 50,000-dalton actin filament bundling protein from *Dictyostelium* amoebae. *J. Biol. Chem.* 265:2286–2291.

Dharmawardhane, S., M. Demma, F. Yang, and J. Condeelis. 1991. Compartmentalization and actin binding properties of ABP-50: the elongation factor-1 α of *Dictyostelium. Cell Motil. Cytoskel.* 20:279–288.

Durso N.A., and R.J. Cyr. 1994. A calmodulin-sensitive interaction between microtubules and a higher plant homolog of elongation factor-1 α. *Plant Cell.* 6:893–905.

Edmonds B.T., J. Murray, and J. Condeelis. 1995. pH regulation of the F-actin binding properties of *Dictyostelium* elongation factor 1 α. *J. Biol. Chem.* 270: 15222–15230.

Edmonds, B.T., J. Wyckoff, Y.-G. Yeung, Y. Wang, E.R. Stanley, J. Jones, J. Segall, and J. Condeelis. 1996. Elongation factor-1α is an overexpressed actin binding protein in metastatic rat mammary adenocarcinoma. *J. Cell Sci.* 109:2705–2714.

Fesce, R., F. Benfanati, P. Greengard, and F. Valtorta. 1992. Effects of the neuronal phosphoprotein synapsin I on actin polymerization. *J. Biol. Chem.* 267: 11289–11299.

Feynman, R.P., R.B. Leighton, and M. Sands. 1963. The Feynman Lectures on Physics. Vol. 1. Addison-Wesley Publishing Company, Reading, MA. 6-2–6-5.

Furukawa, R., J.E. Wampler, and M. Fechheimer. 1988. Measurement of the cytoplasmic pH of *Dictyostelium discoideum* using a low light level microspectrofluorometer. *J. Cell Biol.* 107:2541–2549.

Furukawa, R., J.E. Wampler, and M. Fechheimer. 1990. Cytoplasmic pH of *Dictyostelium discoideum* amebae during early development: identification of two cell subpopulations before the aggregation stage. *J. Cell Biol.* 110: 1947–1954.

Goldmann, W.H., A. Bremer, M. Haner, U. Aebi, and G. Isengberg. 1994. Native talin is a dumbbell-shaped homodimer when it interacts with actin. *J. Struct. Biol.* 112:3–10.

Greengard, P., F. Valtorta, A.J. Czernik, and F. Benfenati. 1993. Synaptic vesicle phosphoproteins and regualtion of synaptic function. *Science (Wash. DC).* 259:780–785.

Hall, A.L., A. Schlein, and J.C. Condeelis. 1988. Relationship of pseudopod extension to chemotactic hormone-induced actin polymerization in amoeboid cells. *J. Cell. Biochem.* 37:285–299.

Hall, A.L., V. Warren, S. Dharmawardhane, and J. Condeelis. 1989. Identification of actin nucleation activity and polymerization inhibitor in ameboid cells: their regulation by chemotactic stimulation. *J. Cell Biol.* 109:2207–2213.

Kaufmann, S, T.H. Piekenbrock, W.H. Goldman, M. Barmann, and G. Isenberg. 1991. Talin binds to actin and promotes filament nucleation. *FEBS Lett.* 284:187–191.

Kaur, K.J., and L. Ruben. 1994. Protein translation elongation factor-1 α from *Trypanosoma brucei* binds calmodulin. *J. Biol. Chem.* 269:23045–23050.

Kinosian, H.J., L.A. Selden, J.E. Estes, and L.C. Gershman. 1993. Actin filament annealing in the presence of ATP and phalloidin. *Biochemistry.* 32: 12353–12357.

Kislauskis, E.H., X. Zhu, and R.H. Singer. 1994. Sequences responsible for intracellular localization of β-actin messenger RNA also affect cell phenotype. *J. Cell Biol.* 127:441–451.

Lee, S., and T.D. Pollard. 1988. Evaluation of the binding of Acanthamoeba profilin to pyrene-labeled actin by fluorescence enhancement. *Anal. Biochem.* 168:148–155.

Liu, G., B.T. Edmonds, and J. Condeelis. 1996*a*. pH , EF1α and the cytoskeleton. *Trends Cell Biol.* 6:168–171.

Liu, G., J. Tang, B.T. Edmonds, J. Murray, S. Levin, and J. Condeelis. 1996*b*. F-actin sequesters EF-1a from interaction with aminoacyl-tRNA in a pH-dependent reaction. *J. Cell Biol.* 135:953–963.

Lo, S.H., P.A. Janmey, J.H. Hartwig, and L.B. Chen. 1994. Interactions of tensin with actin and identification of its three distinct actin-binding domains. *J. Cell Biol.* 125:1067–1075.

Marin, F.T., and F.G. Rothman. 1980. Regulation of development in *Dictyostelium discoideum.* IV. Effects of ions on the rate of differentiation and cellular response to cyclic AMP. *J. Cell Biol.* 87:823–827.

Nagata, S., K. Iwasaki, and Y. Kaziro. 1976. Interaction of the low molecular weight form of elongation factor 1 with guanine nucleotides and aminoacyl-tRNA. *Arch. Biochem. Biophys.* 172:168–177.

Okazaki, K., and S. Yumura. 1995. Differential association of three actin-bundling proteins with microfilaments in *Dictyostelium* amoebae. *Eur. J. Cell Biol.* 66:75–81.

Pollard, T.D. 1983. Measurement of rate constants for actin filament elongation in solution. *Anal. Biochem.* 134:406–412.

Pollard, T.D., and J.A. Cooper. 1986. Actin and actin-binding proteins. A critical evaluation of mechanisms and functions. *Annu. Rev. Biochem.* 55:987–1035.

Ruddies, R., W.H. Goldmann, G. Isenberg, E. Sackmann. 1993. The viscoelasticity of entangled actin networks: the influence of defects and modulation by talin and vinculin. *Eur. Biophys. J.* 22:309–321

Satre, M., J.B. Martin, and G. Klein. 1986. Methyl phosphonate as a $^{31}$P-NMR probe for intracellular pH measurements in *Dictyostelium* amoebae. *Biochimie (Paris).* 71:941–948.

Schreier, M.H., B. Erni, and T. Staehelin. 1977. Initiation of mammalian protein synthesis. I. Purification and characterization of seven initiation factors. *J. Mol. Biol.* 116:727–753.

Selve, N., and A. Wegner. 1986. Rate constants and equilibrium constants for binding of the gelsolin-actin complex to the barbed ends of actin filaments in the presence and absence of calcium. *Eur. J. Biochem.* 160:379–387.

Shestakova, E.A., L.P. Motuz, A.A. Minin, and L.P. Gavrilova. 1993. Study of localization of the protein-synthesizing machinery along actin filament bundles. *Cell Biol. Int.* 17:409–416.

Shiina, N., Y. Gotoh, N. Kubomura, A. Iwamatsu, and E. Nishida. 1994. Microtubule severing by elongation factor 1 α. *Science (Wash. DC).* 266:282–285.

Slobin, L.I. 1980. The role of eucaryotic elongation factor tu in protein synthesis. *Eur. J. Biochem.* 110:555–563.

Slobin, L.I., and W. Moller. 1976. Characterization of developmentally regulated forms of elongation factor 1 in Artemia salina. *Eur. J. Biochem.* 69: 367–375.

Stapulionis, R., and M.P. Deutscher. 1995. A channeled tRNA cycle during mammalian protein synthesis. *Proc. Natl. Acad. Sci. USA.* 92:7158–7161.

Van Duijn, B., and K. Inouye. 1991. Regulation of movement speed by intracellular pH during *Dictyostelium discoideum* chemotaxis. *Proc. Natl. Acad. Sci. USA.* 88:4951–4955.

Yang, F., M. Demma, V. Warren, S. Dharmawardhane, and J. Condeelis. 1990. Identification of an actin-binding protein from *Dictyostelium* as elongation factor 1α. *Nature (Lond.).* 347:494–496.

Yang, W., W. Burkhart, J. Cavallius, W.C. Merrick, and W.F. Boss. 1993. Purification and characterization of a phosphatidylinositol 4-kinase activator in carrot cells. *J. Biol. Chem.* 268:392–398.

Zambetti, G., L. Wilming, E.G. Fey, S. Penman, J. Stein, and G. Stein. 1990*a*. Differential association of membrane-bound and non-membrane-bound polysomes with the cytoskeleton. *Exp. Cell Res.* 191:246–255.

Zambetti, G., E.G. Fey, S. Penman, J. Stein, and G. Stein. 1990*b*. Multiple types of mRNA-cytoskeleton interactions. *J. Cell Biochem.* 44:177–187.

Zhang, J., R.M. Robson, J.M. Schmidt, and M.H. Stromer. 1996. Talin can crosslink actin filaments into both networks and bundles. *Biochem. Biophys. Res. Commun.* 218:530–537.